JOURNAL OF BACTERIOLOGY, June 2000, p. 3475–3481 Vol. 182, No. 12
0021-9193/00/$04.00+0

Genetic and Phenotypic Analyses of the *rdx* Locus of *Rhodobacter sphaeroides* 2.4.1

JUNG HYEOB ROH AND SAMUEL KAPLAN*

Department of Microbiology and Molecular Genetics, The University of Texas, Health Science Center at Houston, Houston, Texas 77030

Received 9 December 1999/Accepted 21 March 2000

Previously, we reported that *rdxB*, encoding a likely membrane-bound two [4Fe-4S]-containing center, is involved in the aerobic regulation of photosystem gene expression in *Rhodobacter sphaeroides* 2.4.1. To further investigate the role of *rdxB* as well as other genes of the *rdxBHIS* operon on photosystem gene expression, we constructed a series of nonpolar, in-frame deletion mutations in each of the *rdx* genes. Using both *puc* and *puf* operon *lacZ* fusions to monitor photosystem gene expression, under aerobic conditions, in each of the mutant strains revealed significant increased photosynthesis gene expression. In the case of mutations in either *rdxH*, *rdxI*, or *rdxS*, the aerobic induction of photosystem gene expression is believed to be indirect by virtue of a posttranscriptional effect on cbb_3 cytochrome oxidase structure and integrity. For RdxB, we suggest that this redox protein has a more direct effect on photosystem gene expression by virtue of its interaction with the cbb_3 oxidase. An associated phenotype, involving the enhanced conversion of the carotenoid spheroidene to spheroidenone, is also observed in the RdxB, -H, -I, and -S mutant strains. This phenotype is also suggested to be the result of the role of the *rdxBHIS* locus in cbb_3 oxidase activity and/or structure. RdxI is suggested to be a new class of metal transporter of the CPx-type ATPases.

The purple nonsulfur bacterium *Rhodobacter sphaeroides* 2.4.1 is able to grow aerobically as a chemoheterotroph, anaerobically using respiration or fermentation, and photosynthetically in either an autotrophic or heterotrophic mode. When grown under photosynthetic or anaerobic (semiaerobic) conditions, the photosynthetic apparatus including light-harvesting system I (B875), light-harvesting system II (B800-850), bacteriochlorophyll *a* (Bchl), and carotenoids (Crts) are synthesized and localized to the intracytoplasmic membrane (16).

Our previous results have shown that the cbb_3 cytochrome oxidase (29, 31, 40) and the apparently membrane-bound RdxB (29) as well as known regulatory elements such as FnrL (39, 41), the PrrBA two-component activation system (6, 7, 8, 32), the AppA/PpsR antirepressor/repressor system (11, 12), and the outer membrane-localized TspO protein (37) are involved in the regulation of photosystem formation. It has been suggested that a redox signal originating from the cbb_3 cytochrome oxidase normally acts to inhibit photosystem gene expression under aerobic conditions, most likely acting through the two-component activation system, PrrBA (30, 31).

This same redox flow through the cbb_3 cytochrome oxidase also plays a role in controlling the relative accumulation of Crt, mainly spheroidene (SE) and spheroidenone (SO), under photosynthetic conditions (29, 30, 31, 38, 40). These studies also implicated the *rdxB* gene as being involved in the regulation of photosynthesis gene expression and Crt accumulation (29, 31). The *rdxBHIS* operon of *R. sphaeroides* 2.4.1 was initially identified through the discovery of *rdxB* as a homologue of the *rdxA* gene (25), which encodes a membrane-localized redox protein apparently containing two [4Fe-4S] clusters.

The *rdxBHIS* operon maps immediately downstream of the *ccoNOQP* operon, which encodes the cbb_3 cytochrome oxidase. This oxidase consists of four subunits: CcoN, to which heme *b* and copper cofactors are bound; CcoO (monoheme cytochrome *c*); CcoQ (signal transponder protein); and CcoP (diheme cytochrome *c*) (10, 22, 24, 31). Microorganisms which contain a *ccoNOQP*/*fixNOQP* operon encoding a cbb_3 cytochrome oxidase are also reported to possess the *rdxBHIS*/*fixGHIS* operon at the 3′ end of the *ccoNOQP* operon (5, 14, 21, 22, 29, 33).

Because of the apparent relationship of the *rdxB* locus to the O_2-sensing signal transduction pathway involving the cbb_3 cytochrome oxidase, as well as the relative abundance of the Crts SE and SO, we have undertaken a genetic and phenotypic study of each gene of the *rdxBHIS* locus. To facilitate this analysis, we have constructed nonpolar, in-frame deletion mutations in each of the *rdx* genes in order to ascertain the role(s) of each of the subunits.

MATERIALS AND METHODS

Bacterial strains, plasmids, and growth conditions. The *R. sphaeroides* and *Escherichia coli* strains and plasmids used in this study are described in Table 1. *E. coli* strains were grown at 37°C on Luria-Bertani medium supplemented, when required, with tetracycline (20 μg/ml) and ampicillin, kanamycin, streptomycin, and spectinomycin (each at 50 μg/ml). *R. sphaeroides* strains were grown at 30°C on Sistrom's minimal medium A (SIS) containing succinate as a carbon source (3). Final concentrations of antibiotics were 1 μg/ml for tetracycline and 50 μg/ml for kanamycin, trimethoprim, spectinomycin, and streptomycin. Aerobic cultures were grown on a rotary shaker or sparged with 30% O_2–69% N_2–1% CO_2. Photosynthetic cultures were grown at a light intensity of 50 W/m^2 and sparged with 95% N_2–5% CO_2. Semiaerobic cultures were sparged with 2% O_2–1% CO_2–97% N_2. Strains grown anaerobically in the dark were cultured in SIS supplemented with 0.1% yeast extract in the presence of 60 mM dimethyl sulfoxide (DMSO).

DNA manipulation and analysis. Cosmid pUI8180 was digested with *Pst*I, which contains a recognition site upstream of the *ccoP* gene but no recognition sequence within the *rdxBH* genes. The digest was analyzed by Southern hybridization using the PCR-amplified *rdxH* gene as a probe. A specific 4.8-kb DNA fragment encompassing the entire *rdxBHIS* operon was observed following exposure of the probed gel to X-ray film (data not shown). The *Pst*I fragment corresponding to this band was subcloned into the same site of pBluescript II KS+ and designated pJR101 (Fig. 1). The plasmid, pJR101, which was used for sequencing template DNA contained a portion of the *ccoP* gene, the entire *rdxBHIS* operon, and a downstream 148-bp flanking region.

* Corresponding author. Mailing address: Department of Microbiology and Molecular Genetics, The University of Texas, Health Science Center at Houston, 6431 Fannin St., Houston, TX 77030. Phone: (713) 500-5502. Fax: (713) 500-5499. E-mail: skaplan@utmmg.med.uth.tmc.edu.

TABLE 1. Bacterial strains and plasmids used in this study

Strain or plasmid	Relevant characteristic(s)	Reference or source
E. coli		
DH5α*phe*	DH5α*phe*::Tn*10d*Cm	6
S17-1	C600::RP4-2(Tc::Mu)(Km::Tn7) *thi pro hsdR recA* Tra^+	35
R. sphaeroides		
2.4.1	Wild type	W. Sistrom
RDXBΔ	2.4.1 derivative, in-frame deletion in *rdxB*	31
CCONΔ	2.4.1 derivative, in-frame deletion in *ccoN*	31
JR112	2.4.1 derivative, in-frame deletion in *rdxH*	This study
JR114	2.4.1 derivative, in-frame deletion in *rdxS*	This study
JR117	2.4.1 derivative, in-frame deletion in *rdxI*	This study
Plasmid		
pBluescript SK+	Ap^r *lacPOZ′*	Stratagene
pRK415	Tc^r Mob^+ *lacZ*α IncP	15
pBBR1MCS2	Km^r	18
pLO1	Km^r *sacB* RP4-*oriT* ColE1-*oriV*	20
pUI8180	Cosmid containing *rdxBHIS* operon	39
pCF200Km	Sp^r St^r Km^r IncQ *puc*::*lacZYA′*	19
pUI1663	Sp^r St^r Km^r IncQ *puf*::*lacZYA*	8
pJR101	pBluescript SK+ :: 4.9-kb *Pst*I fragment containing *rdxBHIS* operon	This study
pJR104	pLO1::1.8-kb *Fsp*I + *Hin*cII fragment containing in-frame deleted *rdxI*	This study
pJR106	pLO1::1.1-kb *Ssp*I + *Hin*cII fragment containing in-frame deleted *rdxH*	This study
pJR107	pLO1::1.7-kb *Nru*I fragment containing in-frame deleted *rdxS*	This study
pJR115	pBBR1MCS2::0.6-kb *Sac*II fragment containing *rdxS* gene	This study
pJR116	pBBR1MCS2::1.1-kb *Xba*I + *Sac*I fragment containing *rdxH* gene	This study
pJR120	pBBR1MCS2::2.7-kb *Kpn*I + *Hin*dIII fragment containing *rdxI* gene	This study
pJR121	pBBR1MCS2::2.1-kb *Hin*dIII + *Sac*II fragment containing *rdxB* gene	This study

Conjugation techniques. Plasmids were mobilized by biparental or triparental mating from *E. coli* strains into *R. sphaeroides* strains as described elsewhere (4).

Construction of *rdxBHIS* in-frame deletion mutations. The method and mutant selection for the *rdxB* in-frame deletion mutation were previously reported (31). Below we describe the methods for constructing the *rdxHIS* in-frame deletion mutations.

(i) *rdxH* mutation. A 1.05-kb *Aat*II-*Sac*I fragment containing the *rdxH* gene from pJR101 (Fig. 1) was subcloned into the same site of pUC19 and designated pH1. Plasmid pH1 was used as template DNA for PCR to construct the *rdxH* in-frame deletion mutation. The PCR was performed with primers 18Reverse (5′-AGC GGA TAA CAA TTT CAC ACA GGA-3′) and MURDXH (5′-CCC CGC GGA GCC TGA GTT CGT GCT G-3′) to generate a DNA fragment with a 57-bp in-frame deletion (amino acid residues 89 to 107). The PCR-amplified DNA fragment was digested with *Sac*II-*Sph*I and inserted at the same site of pH1, yielding plasmid pH2. DNA sequencing of the PCR-amplified region of plasmid pH2 was performed to confirm the in-frame deletion as well as the absence of any additional mutations. Plasmid pH2 was blunt ended with *Ssp*I-*Hin*cII and then cloned into the *Pme*I site of the suicide vector, pLO1 (20). The lengths of the flanking DNA regions for homologous recombination were approximately 460 and 580 bp. The resulting plasmid, pJR106, was transferred to *R. sphaeroides* 2.4.1 by conjugation, and screening for single and double recombinants was performed as described previously (31). The *rdxH* in-frame deletion mutation was verified by DNA sequencing of the PCR-amplified DNA fragment containing the mutated region.

(ii) *rdxI* mutation. Plasmid pJR101 has four *Sac*I sites; one is derived from pUC19, and the remaining three (at 322, 904, and 1792 bp) are located within the *rdxI* gene (Fig. 1). Plasmid pJR101 was partially digested with 1 U of *Sac*I for 10 min at 37°C and separated by agarose gel electrophoresis. The partially digested, larger DNA fragment was eluted, self-ligated, and transformed to *E. coli* DH5α*phe*. We found one plasmid having the deletion of two *Sac*I fragments

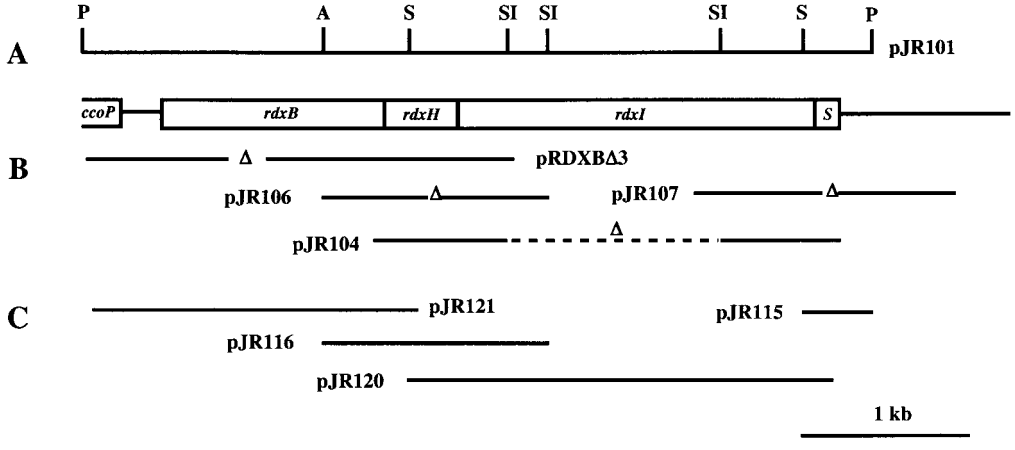

FIG. 1. Physical map of the *R. sphaeroides* 2.4.1 *rdxBHIS* operon. (A) Important restriction sites used in this study (P, *Pst*I; A, *Aat*II; S, *Sac*II; SI, *Sac*I) are shown. (B) Plasmids used in construction of the in-frame deletion mutants. Deleted regions are represented by Δ. (C) Chromosomal fragments used to complement the *rdxB*, *rdxH*, *rdxI*, and *rdxS* mutants. All DNA fragments were introduced in plasmid pBBR1MCS2 (18). Each gene of the *rdxBHIS* operon was expressed from the kanamycin resistance gene promoter on the plasmid.

(corresponding to amino acids 108 to 597). This plasmid was blunt ended with *Fsp*I-*Hinc*II and cloned into the *Pme*I site derived from pLO1 (20). Mutant screening for the *rdxI* mutation was performed as described previously (31), and the in-frame deletion was confirmed by sequencing of the PCR-amplified DNA fragment of the RdxI mutant.

(iii) *rdxS* mutation. The 1.6-kb *Acc*I fragment containing *rdxS* of pJR101 was isolated and cloned into the same site of pBluescript II KS+; the resulting plasmid was designated pAC1. The 3′ flanking region of the *rdxS* gene within plasmid pJR101 was 148 bp, which is not sufficient for homologous recombination. We therefore amplified the 3′-terminal flanking region of the *rdxS* gene contained within cosmid pUI8180. The PCR was performed with primers MURDXS (5′-CCG GAT CCG CGC CAG TAG CAC GCG CTT T-3′) and pLA1 (5′-GGC GCA GGG GAT CA-3′), using cosmid pUI8180 as the template. The PCR product contained the 24-bp deletion (corresponding to amino acids 43 to 50) of the *rdxS* gene. The amplified DNA (about 1,350 bp) was digested with *Bam*HI-*Not*I and exchanged into the same restriction sites of pAC1. A 580-bp *Bam*HI fragment that was deleted by the above-described *Bam*HI treatment used to subclone the PCR product was reintroduced into this plasmid. Finally, an *Nru*I fragment containing the *rdxS* mutation was ligated into *Pme*I-digested pLO1 (20). Mutant screening and confirmation were performed as described above.

Spectral analysis. A crude cell extract was prepared by passage through a French press (Aminco, Urbana, Ill.), followed by two rounds of centrifugation at 13,000 rpm to remove unbroken cells and cell debris. The membrane fraction was prepared by centrifugation at 100,000 × *g* for 1 h. The dithionite-reduced-minus-oxidized spectrum was recorded with 200 μg of membrane protein dissolved in Tris buffer (pH 7.5) containing 0.5% dodecyl maltoside. The sample was reduced for 2 min after adding 30 μl of 15% (wt/vol) sodium dithionite. The amounts of *b*- and *c*-type hemes were estimated by using the extinction coefficients $\varepsilon_{561\text{-}575}$ of 22 mM^{-1} cm^{-1} and $\varepsilon_{551\text{-}540}$ of 19 mM^{-1} cm^{-1}, respectively. The amount of B800-850 and B875 light-harvesting complexes was determined as described elsewhere (23). Photopigments were extracted from cell pellets with acetone-methanol (7:2, vol/vol) mixture and quantitated as described previously (3). The extracted mixture was concentrated for high-pressure liquid chromatography (HPLC) analysis on a Shimadzu system equipped with an SPD-M10AV diode array detector as previously described (38). All analyses were performed in duplicate at least twice, and the data presented are the averages of the values obtained.

Enzyme assay and protein determination. Assays of β-galactosidase and cbb_3 cytochrome oxidase activity were performed on crude cell extracts of *R. sphaeroides* as previously described (31) at least twice, with standard deviations not exceeding 15%. Protein concentrations were determined with the Pierce (Rockford, Ill.) bicinchoninic acid protein assay reagent with bovine serum albumin as a standard. Sodium dodecyl sulfate-polyacrylamide gel electrophoresis of protein present in the membrane fraction was performed in a Tris-glycine-sodium dodecyl sulfate buffer system using a mini-slab gel apparatus. Western analysis was carried out as described previously (37), using rabbit anti-CcoO and anti-CcoP antibodies at a 1:5,000 dilution. Blots were then incubated with alkaline phosphatase-coupled goat anti-rabbit immunoglobulin G (1:10,000 dilution) and developed using nitroblue tetrazolium and 5-bromo-4-chloro-3-indolylphosphate. The specific band which appeared on the membrane was scanned and quantitated using the NIH Image 1.61 software.

Nucleotide sequence accession number. The nucleotide sequence of the *rdxBHIS* operon was submitted to GenBank (accession no. AF202779).

RESULTS

DNA sequence of the *rdxBHIS* operon. The *rdxBHIS* operon was partially sequenced in a previous study (29). In this study, we sequenced the remaining *rdxI*, *rdxS*, and flanking regions, which were contained within cosmid pUI8180, in addition to the previously reported *rdxBHI′* region (29). Derived proteins homologous to *rdxBHIS* are reported for the phylogenetically related species *Rhodobacter capsulatus* (17), *Bradyrhizobium japonicum* (33), *Rhizobium leguminosarum* (GenBank accession no. AJ001522), and *Rhizobium meliloti* (14) (Table 2).

All Rdx components are apparently membrane proteins containing at least one membrane-spanning region (25, 29). Comparative amino acid sequence alignments of *rdxI* show that all of the putative functional regions of recently suggested CPx-type ATPases, such as a metal binding domain (C53-X-X-C56), a portion of a phosphatase domain (T308-G-E310), an ion transduction domain (C413-P-C415), E1-E2 ATPase phosphorylation sites (D457-K-T-G-T461), an ATP binding region (V634-G-D-G637), and eight putative transmembrane regions, are present (2, 14, 27, 33, 34, 36). RdxS, consisting of 52 amino acids, possesses no recognizable protein motifs.

TABLE 2. Amino acid sequence identity of RdxI and RdxS homologous proteins

Protein[a]	% Identity							
	R. capsulatus		*B. japonicum*		*R. leguminosarum*		*R. meliloti*	
	CcoI	CcoS	FixI	FixS	FixI	FixS	FixI	FixS
RdxI	74.1		45.4		45.5		45.0	
RdxS		70.6		57.8		57.1		57.1

[a] RdxI and RdxS of *R. sphaeroides* 2.4.1. CcoI/FixI and CcoS/FixS sequences of *R. capsulatus* (17), *B. japonicum* (33), *R. leguminosarum* (GenBank accession no. AJ001522), and *R. meliloti* (14) were used for analysis.

Construction of in-frame deletion mutations. The plasmids used in construction of the in-frame deletion mutations for each of the genes of *rdxHIS* are depicted in Fig. 1B. We also show construction of the *rdxB* mutation as described elsewhere (31).

All mutations of the *rdxBHIS* locus gave rise to colonies with increased red pigmentation on SIS plates in the presence of O_2 compared to the wild type, 2.4.1, as previously reported for *rdxB* (29, 30, 31). This suggested the induction of photosynthesis genes in the presence of O_2. In particular, in-frame mutations of *rdxI* and *rdxS* formed very dark red, very small colonies compared with the wild type. The colony sizes of *rdxB* and *rdxH* in-frame mutations were between those of the wild type, 2.4.1, and the RdxI and RdxS mutants on SIS plates. However, colony pigmentation of the *rdxB* in-frame mutation was substantially darker red than that of the *rdxH* mutation.

Complementation of Rdx mutants. Complementation experiments were performed to ensure that each of the Rdx mutants possessed a specific in-frame deletion and that no additional extragenic mutations were present. The plasmids used for complementation are depicted in Fig. 1C. Each of the gene products was expressed from the kanamycin resistance gene promoter on plasmid pBBR1MCS2 (18). Complementation was determined by measurements of the Crt composition under phototrophic conditions, growth characteristics, and colony pigmentation. When complemented mutants were cultured photosynthetically, all mutant strains were reverted to the wild-type, green-brown coloration from the red pigmentation due to an excess of SO over SE (Fig. 2). The SE/SO ratio was also similar to that obtained with the wild type 2.4.1 (Fig. 2). When the complemented mutant strains were cultured under semiaerobic conditions, growth was restored to that of the wild type (data not shown). This complementation analysis also demonstrated that none of the in-frame deletions were polar on the downstream gene(s) of the *rdx* operon.

Therefore, these results revealed that each Rdx mutant contained a mutation in the designated gene only.

Growth of Rdx mutants. We next examined the growth characteristics and quantitated the levels of spectral complex formation under highly aerobic, semiaerobic, and photoheterotrophic conditions in order to more fully characterize each of the mutant strains. Although highly aerobic growth patterns of the mutants (Fig. 3A) were similar to one another and to the wild-type patterns (doubling time of approximately 3 h), growth under semiaerobic conditions revealed a different response (Fig. 3B). In-frame mutations of either *rdxI* and *rdxS* showed approximately 50% of the growth rate (doubling time of 9 to 10 h) of RdxB, RdxH, and wild-type strains (3 to 5 h) under semiaerobic conditions. Thus, we assumed that RdxI and RdxS might have a more significant physiological role under conditions of low O_2 tensions.

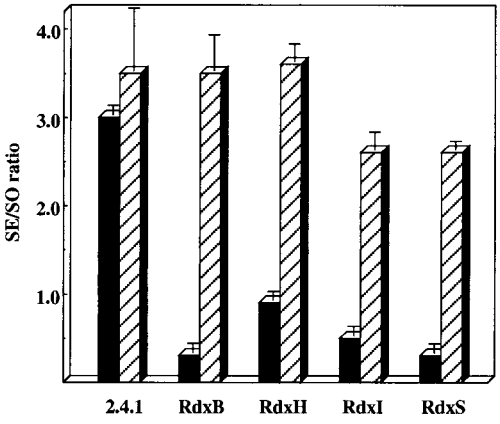

FIG. 2. Complementation of *rdxBHIS* in-frame deletion mutants. Carotenoid composition (SE/SO ratio) of the wild-type strain, 2.4.1, and mutant strains was analyzed by HPLC as described in Materials and Methods. Strains were grown photosynthetically at a light intensity of 50 W/m^2. Data are the mean values of two independent cultures. Dark blocks represent 2.4.1 and each of the *rdxBHIS* mutants; hatched blocks represent the complemented strain. Plasmid pBBR1MCS2 (18) was used to complement 2.4.1.

Spectral complex analysis under aerobic conditions. It has been shown that spectral complex formation of *R. sphaeroides* 2.4.1 under aerobic conditions can be controlled by the cellular redox poise through the cbb_3 terminal oxidase (29, 30, 31, 38, 40). These earlier studies also revealed that the *rdxB* gene was somehow involved in this response (29, 31). To begin to understand the role, if any, of each of the other *rdx* genes, we analyzed the spectral complex content of each mutant strain grown under highly aerobic conditions.

The mutant strains exhibited 3- to 7-fold and 7- to 13-fold increased levels of the B800-850 and B875 complexes, respectively (Table 3). The levels of total Crt (two- to fourfold) and Bchl (four- to ninefold) were also higher in all mutant strains than in the wild-type strain, 2.4.1. All Rdx mutants possessed SO as the major Crt under phototrophic conditions, with the level of SE being substantially lower than that in the wild type. The higher amounts of the B875 complex compared to the B800-850 complex are the result of low Bchl availability under aerobic conditions and its preferential use for B875 assembly relative to B800-850 assembly, as reported earlier (13, 26, 31, 38).

TABLE 3. Spectral complex formation of *R. sphaeroides* strains grown under aerobic conditions

Mutation[a]	Spectral complex formation[b]			
	B800-850	B875	Crt	Bchl
None (2.4.1)	<0.1	0.3 ± 0.1	0.6 ± 0.2	0.6 ± 0.2
rdxB	0.3 ± 0.1	2.0 ± 0.1	1.1 ± 0.1	2.4 ± 0.2
rdxH	0.5 ± 0.1	3.2 ± 0.1	1.6 ± 0.1	4.1 ± 0.3
rdxI	0.5 ± 0.1	3.3 ± 0.3	2.0 ± 0.1	5.2 ± 0.1
rdxS	0.7 ± 0.1	3.9 ± 0.2	2.1 ± 0.2	5.4 ± 0.4

[a] Strains were grown by sparging with 69% N_2–30% O_2–1% CO_2 to an optical density at 600 nm of 0.3.

[b] B800-850 and B875 spectral complexes are expressed as nanomoles per milligram of protein. Bchl and Crt are expressed as micrograms per 100 ml of culture.

Analysis of *puc* and *puf* operon expression in Rdx mutants. The relationship between the formation of spectral complexes in the presence of O_2 and the actual expression of the *puc* and *puf* genes in the *rdxB* polar insertion mutation was reported previously (29). In these earlier experiments, transcription levels of the genes encoding the B800-850 and B875 apoproteins were approximately 13.5- and 4.3-fold, respectively, higher than in the wild type, 2.4.1.

To extend these analyses to each of the *rdx* genes described here, promoter activities of the *puc* and *puf* genes under aerobic conditions were determined. As shown in Table 4, the level of *puc* operon expression was increased approximately 4.1- to 6.5-fold in the different Rdx mutants compared with the wild type. The values for *puf* operon expression also increased approximately 2.8- to 5.0-fold in the mutant strains. Thus, all of the *rdx* in-frame deletion mutations when present individually gave rise to the derepression of both the *puc* and *puf* operons under aerobic conditions.

Spectral complex analysis under anaerobic conditions. When wild type 2.4.1 is grown under dark, dimethyl sulfoxide (DMSO) conditions, pigmentation is the typical green-brown color resulting from the highly expressed Crt, SE, in the presence of Bchl. Under these conditions, the SE-to-SO ratio of 2.4.1 is 5.1 ± 0.8. However, differences in pigmentation were found when the individual RdxB, -I, and -S mutants (1.8 ± 0.1, 1.8 ± 0.1, 1.9 ± 0.1, respectively) were grown under dark, DMSO conditions, in which they appeared red. Only the RdxH mutant showed the green-brown pigmentation similar to that of the wild type, 2.4.1, with an SE/SO ratio of 4.2 ± 0.5. The

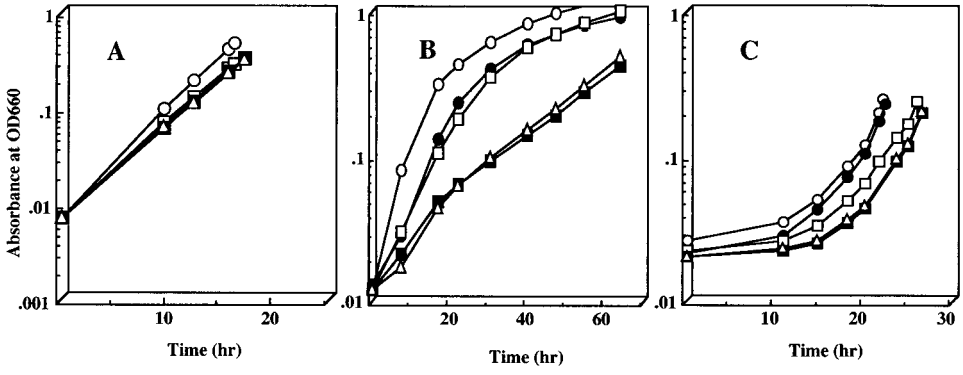

FIG. 3. Relative growth rates of mutant strains under aerobic conditions (A; sparged with 30% O_2–1% CO_2–69% N_2), semiaerobic conditions (B; sparged with 2% O_2–1% CO_2–97% N_2), and phototrophic conditions (C; sparged with 5% CO_2–95% N_2). ○, wild type; ●, *rdxB*; □, *rdxH*; ■, *rdxI*; △, *rdxS*; ▲, *ccoN*. OD660, optical density at 660 nm.

TABLE 4. β-Galactosidase activities from cell extracts of *R. sphaeroides* strains containing *puc*::*lacZ* (pCF200Km) or *puf*::*lacZ* (pUI1663) fusion plasmid

Mutation[a]	β-Galactosidase activity (nmol/min/mg of protein)[b]	
	puc::*lacZ*	*puf*::*lacZ*
None (2.4.1)	221 ± 24	279 ± 15
rdxB	980 ± 12	769 ± 30
rdxH	1,427 ± 1	1,291 ± 99
rdxI	1,187 ± 28	1,381 ± 38
rdxS	900 ± 12	927 ± 43

[a] Strains were grown aerobically with sparging of 69% N_2–30% O_2–1% CO_2 to an A_{600} of 0.2.
[b] Average of two independent experiments.

result observed for the RdxH mutant is similar to that observed for the CcoQ mutant of the cbb_3 cytochrome oxidase (31) and the PrrC mutant (9), both of which are defective in being able to transduce the inhibitory signal from cbb_3 cytochrome oxidase to the membrane-bound histidine kinase, PrrB.

***cbb*$_3$ cytochrome oxidase activity in the Rdx mutants.** The *rdxBHIS* operon is located immediately 3′ to the *ccoNOQP* operon, which encodes the cbb_3 cytochrome oxidase (29, 39). Because the RdxI and RdxS mutants showed slow growth under semiaerobic conditions, in which the cbb_3 cytochrome oxidase is the major terminal oxidase (10, 21), we investigated both cbb_3 cytochrome oxidase activity and the levels of the CcoO and CcoP proteins by Western blot analysis in each of the Rdx mutants. Previously, it was shown that with a *ccoN* in-frame deletion mutation grown under anaerobic conditions with DMSO, cbb_3 oxidase activity was undetectable (31). All of the individual RdxB, -H, -I, and -S mutants together with the wild type 2.4.1 and the CcoN mutant as a control were grown under anaerobic dark, DMSO conditions, and cbb_3 cytochrome oxidase activity was measured. This is the only terminal oxidase which is measurable under these conditions (31). As shown in Fig. 4A, the RdxB mutant had at least the same level of cbb_3 oxidase activity as 2.4.1, while levels for mutants RdxH, RdxI, and RdxS were substantially lower. When the individual Rdx mutants were grown under photosynthetic conditions in SIS medium, cbb_3 cytochrome oxidase activity was reduced even further to near background levels except for that of the RdxB mutant, which was at or greater than wild-type levels. In no case was the reduction in cbb_3 oxidase activity quite as pronounced as in the CcoN mutant (31).

To ascertain if the observed cbb_3 activity reflected the amounts of cbb_3 protein in the cell, we performed Western blot analysis using a CcoO/P-specific antiserum made against the *R. sphaeroides* 2.4.1 polypeptides (Fig. 4B). While the CcoO/P-specific signal is abundant in the wild type 2.4.1 and the RdxB mutant to approximately the same extent, reduced levels of these polypeptides were present in the membrane fractions isolated from the RdxH, RdxI, and RdxS mutant strains. However, the loss of cbb_3-specific oxidase activity is clearly in excess of the residual levels of P and O polypeptides in the membrane.

The dithionite-reduced-minus-air-oxidized spectra of the membrane fractions of each of the Rdx mutants showed both the *b*- and *c*-type cytochromes (Fig. 5). Amounts of the *b* ($\varepsilon_{561\text{-}575}$) and *c* ($\varepsilon_{551\text{-}540}$) cytochromes were similar when 2.4.1 and the RdxB mutant were compared. When the levels of the cytochromes in the RdxH, -I, and -S mutants were quantitated, the *b* type was reduced 33.9% in all of the mutants and the *c* type was reduced 47.3, 44.6, and 45.9%, respectively. These

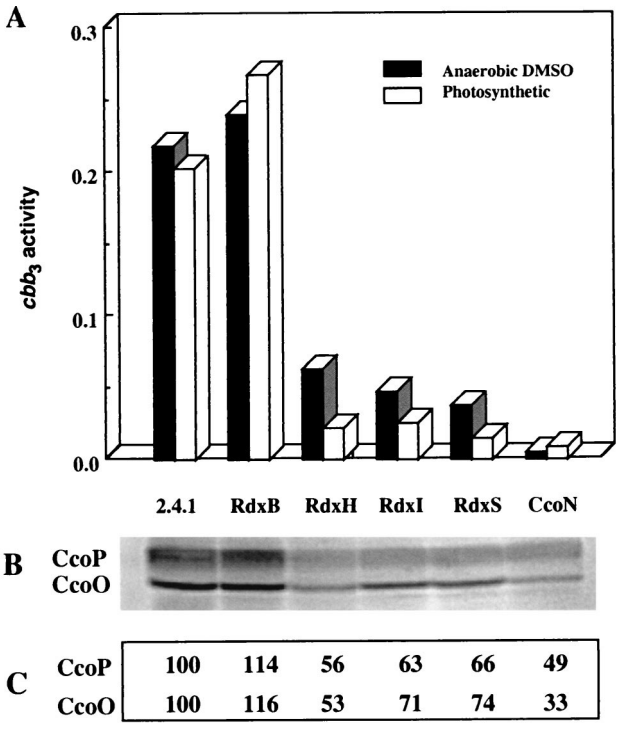

FIG. 4. Activities and Western blot analysis of cbb_3 cytochrome oxidase of *R. sphaeroides* 2.4.1 and mutant strains. (A) Strains were cultured under anaerobic dark, DMSO conditions (■) and under photosynthetic conditions (□). cbb_3 oxidase activity was expressed as micromoles per minute per milligram of protein. (B) Western blot analysis was performed with 30 μg of membrane fraction from cells grown under anaerobic dark, DMSO conditions using *R. sphaeroides* CcoO/P-specific antibody. (C) Quantitation of protein levels by Western blotting. Quantitation was performed by subtracting the background levels for each lane from the specific band. The CcoP and CcoO levels of 2.4.1 were considered 100%, and others are given relative to that value.

values are in relatively good agreement with the Western blot data provided earlier. Therefore, it is safe to conclude that the cbb_3 oxidase activity is more severely affected than the physical presence of the component polypeptides within the membrane in these mutant strains.

Finally, to determine whether the effect observed for each of the Rdx mutants on cbb_3 activity was at the transcriptional or posttranscriptional level, the promoter activity of the *cco* operon was determined using a *lacZ* transcriptional fusion (24) under semiaerobic conditions. We observed that similar β-galactosidase activities were found in the wild type, 2.4.1, and all of the Rdx mutant strains, implying that the lower levels of cbb_3 activity in the mutants was not the result of a transcriptional effect on the levels of *cco* operon expression (data not shown).

DISCUSSION

Photosystem gene expression in *R. sphaeroides* 2.4.1 is dependent on a variety of environmental conditions, such as O_2 tension and light intensity (16). Studies from our laboratory have shown that *R. sphaeroides* 2.4.1 possesses at least four regulatory systems which mediate O_2- and/or light-dependent control of photosystem gene expression (6, 7, 8, 9, 11, 12, 37, 39, 41). In addition to these regulatory systems, mutations in the *ccoNOQP* operon encoding the cbb_3 cytochrome oxidase (29, 31, 40) and in the *rdxB* gene (29, 31) result in the O_2-insensitive formation of the photosystem as well as altered Crt

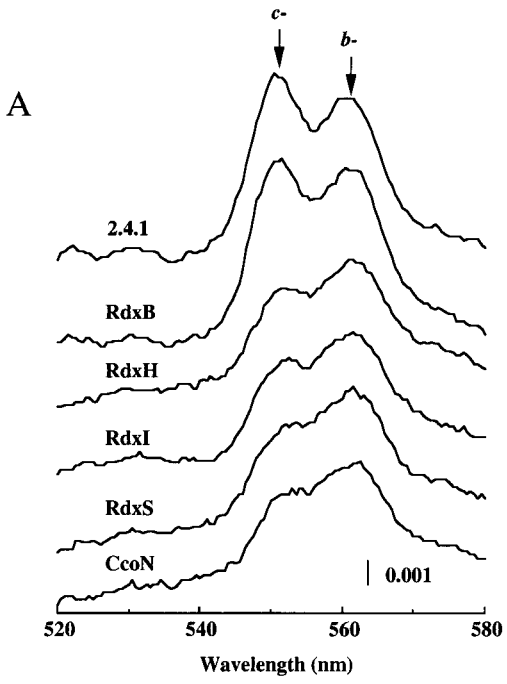

B

	2.4.1	RdxB	RdxH	RdxI	RdxS	CcoN
b-	100	105.1	66.1	66.1	66.1	55.9
c-	100	105.3	52.7	55.4	54.1	46.0

FIG. 5. Reduced-minus-oxidized spectra of *R. sphaeroides* strains (A) and the *b*- and *c*-type cytochrome content in the membrane fraction (B). The strains were grown under semiaerobic conditions (sparged with 2% O_2–1% CO_2–97% N_2); 200 μg of total membrane protein was used. The *b*-type (0.39 μM^{-1} cm^{-1}) and *c*-type (0.27 μM^{-1} cm^{-1}) cytochrome content of 2.4.1 was considered 100%, and the contents of Rdx mutants are given relative to that value.

accumulation. It was proposed that these membrane-associated complexes are involved in generating and/or transmitting a signal to the membrane-localized PrrB histidine kinase, preventing its activation of the PrrA response regulator, which is required for photosystem gene expression (8, 30, 31). Unlike the well-studied cbb_3 cytochrome oxidase gene, the *rdxBHIS* genes have not been characterized.

Previously, we reported that a polar insertion into *rdxB* (29) as well as an in-frame deletion mutation within *rdxB* (31) activates photosystem gene expression in the presence of high O_2. To further understand the role of all genes of the *rdxBHIS* operon in this signal transduction pathway, we have constructed a series of in-frame deletion mutations which are nonpolar for each of the *rdx* genes.

On the basis of the data presented here and in consideration of our earlier results for RdxB mutant strains in our studies of the cbb_3 oxidase, mutants of RdxB more closely resemble the wild type 2.4.1 than do any of the other Rdx mutants in terms of growth rate, cbb_3 cytochrome oxidase activity, levels of the CcoO and CcoP proteins, and reduced-minus-oxidized spectra. Thus, the effects of nonpolar mutations in *rdxB* are limited to the activation of photosynthesis gene expression in the presence of O_2 and an alteration in the ratio of SE to SO.

Conversely, the RdxH, -I, and -S mutant strains are appreciably different from the wild type, 2.4.1, and the RdxB mutant in that they show reduced growth rates, reduced levels of cbb_3 oxidase activity, and reduced levels of the CcoO and CcoP polypeptides and *b*- and *c*-type cytochromes. On the other hand, like the RdxB mutant, they show increased photosynthesis gene expression in the presence of O_2, and with one notable exception (see below), they show altered ratios of SE to SO.

Even within this latter grouping, the RdxH mutant does not appear to be as severely affected as the RdxI and -S mutant strains. For example, the SE-to-SO ratio of the RdxH mutant grown under dark, DMSO conditions is virtually normal, in contrast to the very abnormal ratio when this same mutant is grown photosynthetically. Thus, the RdxH mutant appears to possess the most complex phenotype.

Because of the relatively severe diminution of cbb_3 oxidase activity but otherwise modest loss of CcoO and CcoP polypeptide levels in the RdxH, -I, and -S mutants, we can speculate that the *rdx* gene products play some role in developing and/or maintaining the integrity of the cbb_3 oxidase. Further supportive of this hypothesis is the observation that RdxI possesses features highly similar to those of the metal-transporting CPx-type ATPases by virtue of amino acid sequence homologies (2, 27, 33, 36). The reported features of CPx-type ATPases are well conserved in the RdxI subunit, although we have not determined the number and topology of the transmembrane regions experimentally. Despite these similarities, the operon structures for P-type ATPases from *Enterococcus hirae* (27), *Helicobacter pylori* (2), and *Helicobacter felis* (2) are completely different from the *R. sphaeroides* 2.4.1 *rdxBHIS* operon structure (29). The operon *copYZAB* of *E. hirae* encoding two P-type ATPases (CopAB), a repressor (CopY), and an activator (CopZ) is a well-studied operon of this enzyme class which functions to maintain copper homeostasis (27, 28). The RdxI/FixI type of CPx-type ATPases might represent a new subfamily of these ATPases (14, 17, 21, 29, 33) that probably functions to maintain the activity of the cbb_3 cytochrome oxidase through the maintenance of intracellular copper homeostasis (Fig. 4) (1, 33, 42). Therefore, we suggest that RdxI of *R. sphaeroides* 2.4.1 functions as a specific Cu transporter to and for the cbb_3 cytochrome oxidase (Fig. 4).

RdxS is a small protein of approximately 6 kDa that is thought to be a membrane protein by virtue of its N-terminal region. Our results revealed that the phenotype of the RdxS mutant was most similar to that of the RdxI mutant. As discussed above, the RdxH mutant is the most complex, but because it more closely resembles the RdxI and -S mutant strains, we believe that it is also likely to be involved in making copper available to the cbb_3 oxidase. However, because residual cbb_3 oxidase activity as well as polypeptides are present in the RdxH, -I, and -S mutant strains compared to a CcoN mutant, other Cu transporters and a chaperone system must be available to satisfy the needs of the cbb_3 oxidase, at least in part. Because the physical presence of the CcoO and CcoP polypeptides and the *b*- and *c*-type cytochromes is far in excess of the residual cbb_3 activity, the data suggest that copper availability is not essential for the targeting of these subunits to the membrane but is required for activity.

Finally, because the RdxB mutant is defective only in the activation of photosynthesis gene expression in the presence of O_2 and in the maintenance of the hypothesized 2-oxo donor to SE, in the reduced state (31, 38), we speculate that the RdxB protein can receive reducing equivalents from the cbb_3 cytochrome oxidase, and thus mutants of RdxB can alter the flow of reductant through cbb_3 oxidase in the presence of O_2, resulting in photosynthesis gene expression. In the absence of

O_2, absence of RdxB would result in the excessive production of the 2-oxo donor, causing an accumulation of SO.

ACKNOWLEDGMENT

This work was supported by grant GM15590 to S.K.

REFERENCES

1. **Batut, J., and P. Boistard.** 1994. Oxygen control in *Rhizobium*. Antonie Leeuwenhoek **66:**129–150.
2. **Bayle, D., S. Wangler, T. Weitzenegger, W. Steinhilber, J. Volz, M. Przybylski, K. P. Schafer, G. Sachs, and K. Melchers.** 1998. Properties of the P-type ATPases encoded by the *copAP* operons of *Helicobacter pylori* and *Helicobacter felis*. J. Bacteriol. **180:**317–329.
3. **Cohen-Bazire, G., W. R. Sistrom, and R. Y. Stanier.** 1957. Kinetic studies of pigment synthesis by non-sulfur purple bacteria. J. Cell. Comp. Physiol. **49:**25–68.
4. **Davis, J., T. J. Donohue, and S. Kaplan.** 1988. Construction, characterization, and complementation of a Puf$^-$ mutant of *Rhodobacter sphaeroides*. J. Bacteriol. **170:**320–329.
5. **de Gier, J. W., M. Schepper, W. N. Reijnders, S. J. van Dyck, D. J. Slotboom, A. Warne, M. Saraste, K. Krab, M. Finel, A. H. Stouthamer, R. J. van Spanning, and J. van der Oost.** 1996. Structural and functional analysis of aa_3-type and cbb_3-type cytochrome *c* oxidases of *Paracoccus denitrificans* reveals significant differences in proton-pump design. Mol. Microbiol. **20:** 1247–1260.
6. **Eraso, J. M., and S. Kaplan.** 1994. *prrA*, a putative response regulator involved in oxygen regulation of photosynthesis gene expression in *Rhodobacter sphaeroides*. J. Bacteriol. **176:**32–43.
7. **Eraso, J. M., and S. Kaplan.** 1995. Oxygen-insensitive synthesis of the photosynthetic membranes of *Rhodobacter sphaeroides*: a mutant histidine kinase. J. Bacteriol. **177:**2695–2706.
8. **Eraso, J. M., and S. Kaplan.** 1996. Complex regulatory activities associated with the histidine kinase PrrB in expression of photosynthesis genes in *Rhodobacter sphaeroides* 2.4.1. J. Bacteriol. **178:**7037–7046.
9. **Eraso, J. M., and S. Kaplan.** 2000. From redox flow to gene regulation: the role of the PrrC protein of *Rhodobacter sphaeroides* 2.4.1. Biochemistry **39:**2052–2062.
10. **Garcia-Horsman, J. A., E. Berry, J. P. Shapleigh, J. O. Alben, and R. B. Gennis.** 1994. A novel cytochrome *c* oxidase from *Rhodobacter sphaeroides* that lacks CuA. Biochemistry **33:**3113–3119.
11. **Gomelsky, M., and S. Kaplan.** 1995. *appA*, a novel gene encoding a *trans*-acting factor involved in the regulation of photosynthesis gene expression in *Rhodobacter sphaeroides* 2.4.1. J. Bacteriol. **177:**4609–4618.
12. **Gomelsky, M., and S. Kaplan.** 1997. Molecular genetic analysis suggesting interactions between AppA and PpsR in regulation of photosynthesis gene expression in *Rhodobacter sphaeroides* 2.4.1. J. Bacteriol. **179:**128–134.
13. **Gong, L., J. K. Lee, and S. Kaplan.** 1994. The Q gene of *Rhodobacter sphaeroides*: its role in *puf* operon expression and spectral complex assembly. J. Bacteriol. **176:**2946–2961.
14. **Kahn, D., M. David, O. Domergue, M. L. Daveran, J. Ghai, P. R. Hirsch, and J. Batut.** 1989. *Rhizobium meliloti fixGHI* sequence predicts involvement of a specific cation pump in symbiotic nitrogen fixation. J. Bacteriol. **171:**929–939.
15. **Keen, N. T., S. Tamaki, D. Kobayashi, and D. Trollinger.** 1988. Improved broad-host-range plasmids for DNA cloning in gram-negative bacteria. Gene **70:**191–197.
16. **Kiley, P. J., and S. Kaplan.** 1988. Molecular genetics of photosynthetic membrane biosynthesis in *Rhodobacter sphaeroides*. Microbiol. Rev. **52:**50–69.
17. **Koch, H. G., O. Hwang, and F. Daldal.** 1998. Isolation and characterization of *Rhodobacter capsulatus* mutants affected in cytochrome cbb_3 oxidase activity. J. Bacteriol. **180:**969–978.
18. **Kovach, M. E., R. W. Phillips, P. H. Elzer, R. M. Roop, 2nd, and K. M. Peterson.** 1994. pBBR1MCS: a broad-host-range cloning vector. BioTechniques **16:**800–802.
19. **Lee, J. K., and S. Kaplan.** 1992. Isolation and characterization of *trans*-acting mutations involved in oxygen regulation of *puc* operon transcription in *Rhodobacter sphaeroides*. J. Bacteriol. **174:**1158–1171. (Erratum, **174:**2418.)
20. **Lenz, O., E. Schwartz, J. Dernedde, M. Eitinger, and B. Friedrich.** 1994. The *Alcaligenes eutrophus* H16 *hoxX* gene participates in hydrogenase regulation. J. Bacteriol. **176:**4385–4393.
21. **Mandon, K., P. A. Kaminski, C. Mougel, N. Desnoues, B. Dreyfus, and C. Elmerich.** 1993. Role of the *fixGHI* region of *Azorhizobium caulinodans* in free-living and symbiotic nitrogen fixation. FEMS Microbiol. Lett. **114:**185–189.
22. **Mandon, K., P. A. Kaminski, and C. Elmerich.** 1994. Functional analysis of the *fixNOQP* region of *Azorhizobium caulinodans*. J. Bacteriol. **176:**2560–2568.
23. **Meinhardt, S. W., P. J. Kiley, S. Kaplan, A. R. Crofts, and S. Harayama.** 1985. Characterization of light-harvesting mutants of *Rhodopseudomonas sphaeroides*. I. Measurement of the efficiency of energy transfer from light-harvesting complexes to the reaction center. Arch. Biochem. Biophys. **236:** 130–139.
24. **Mouncey, N. J., and S. Kaplan.** 1998. Oxygen regulation of the *ccoN* gene encoding a component of the cbb_3 oxidase in *Rhodobacter sphaeroides* 2.4.1^T: involvement of the FnrL protein. J. Bacteriol. **180:**2228–2231.
25. **Neidle, E. L., and S. Kaplan.** 1992. *Rhodobacter sphaeroides rdxA*, a homolog of *Rhizobium meliloti fixG*, encodes a membrane protein which may bind cytoplasmic [4Fe-4S] clusters. J. Bacteriol. **174:**6444–6454.
26. **Neidle, E. L., and S. Kaplan.** 1993. 5-Aminolevulinic acid availability and control of spectral complex formation in *hemA* and *hemT* mutants of *Rhodobacter sphaeroides*. J. Bacteriol. **175:**2304–2313. (Erratum, **175:**7123.)
27. **Odermatt, A., H. Suter, R. Krapf, and M. Solioz.** 1993. Primary structure of two P-type ATPases involved in copper homeostasis in *Enterococcus hirae*. J. Biol. Chem. **268:**12775–12779.
28. **Odermatt, A., and M. Solioz.** 1995. Two trans-acting metalloregulatory proteins controlling expression of the copper-ATPases of *Enterococcus hirae*. J. Biol. Chem. **270:**4349–4354.
29. **O'Gara, J. P., and S. Kaplan.** 1997. Evidence for the role of redox carriers in photosynthesis gene expression and carotenoid biosynthesis in *Rhodobacter sphaeroides* 2.4.1. J. Bacteriol. **179:**1951–1961.
30. **O'Gara, J. P., J. M. Eraso, and S. Kaplan.** 1998. A redox-responsive pathway for aerobic regulation of photosynthesis gene expression in *Rhodobacter sphaeroides* 2.4.1. J. Bacteriol. **180:**4044–4050.
31. **Oh, J. I., and S. Kaplan.** 1999. The cbb_3 terminal oxidase of *Rhodobacter sphaeroides* 2.4.1: structural and functional implications for the regulation of spectral complex formation. Biochemistry **38:**2688–2696.
32. **Ouchane, S., and S. Kaplan.** 1999. Topological analysis of the membrane-localized redox-responsive sensor kinase PrrB from *Rhodobacter sphaeroides* 2.4.1. J. Biol. Chem. **274:**17290–17296.
33. **Preisig, O., R. Zufferey, and H. Hennecke.** 1996. The *Bradyrhizobium japonicum fixGHIS* genes are required for the formation of the high-affinity cbb_3-type cytochrome oxidase. Arch. Microbiol. **165:**297–305.
34. **Rensing, C., M. Ghosh, and B. P. Rosen.** 1999. Families of soft-metal-ion-transporting ATPases. J. Bacteriol. **181:**5891–5897.
35. **Simon, R., U. Priefer, and A. Puhler.** 1983. A broad host range mobilization system for in vivo genetic engineering: transposon mutagenesis in Gram negative bacteria. Bio/Technology **1:**37–45.
36. **Solioz, M., and C. Vulpe.** 1996. CPx-type ATPases: a class of P-type ATPases that pump heavy metals. Trends Biochem. Sci. **21:**237–241.
37. **Yeliseev, A. A., and S. Kaplan.** 1995. A sensory transducer homologous to the mammalian peripheral-type benzodiazepine receptor regulates photosynthetic membrane complex formation in *Rhodobacter sphaeroides* 2.4.1. J. Biol. Chem. **270:**21167–21175.
38. **Yeliseev, A. A., J. M. Eraso, and S. Kaplan.** 1996. Differential carotenoid composition of the B875 and B800-850 photosynthetic antenna complexes in *Rhodobacter sphaeroides* 2.4.1: involvement of spheroidene and spheroidenone in adaptation to changes in light intensity and oxygen availability. J. Bacteriol. **178:**5877–5883.
39. **Zeilstra-Ryalls, J. H., and S. Kaplan.** 1995. Aerobic and anaerobic regulation in *Rhodobacter sphaeroides* 2.4.1: the role of the *fnrL* gene. J. Bacteriol. **177:**6422–6431.
40. **Zeilstra-Ryalls, J. H., and S. Kaplan.** 1996. Control of *hemA* expression in *Rhodobacter sphaeroides* 2.4.1: regulation through alterations in the cellular redox state. J. Bacteriol. **178:**985–993.
41. **Zeilstra-Ryalls, J. H., and S. Kaplan.** 1998. Role of the *fnrL* gene in photosystem gene expression and photosynthetic growth of *Rhodobacter sphaeroides* 2.4.1. J. Bacteriol. **180:**1496–1503.
42. **Zufferey, R., E. Arslan, L. Thony-Meyer, and H. Hennecke.** 1998. How replacements of the 12 conserved histidines of subunit I affect assembly, cofactor binding, and enzymatic activity of the *Bradyrhizobium japonicum* cbb_3-type oxidase. J. Biol. Chem. **273:**6452–6459.